IAEA
International Atomic Energy Agency

INDC International Nuclear Data Committee

^{209}Bi(n,f) and ^{nat}Pb(n,f) Cross Sections as a New Reference and Extension of the ^{235}U, ^{238}U and ^{239}Pu(n,f) Standards up to 1 GeV

Benjaminas Marcinkevicius, Stanislav Simakov

IAEA Nuclear Data Section
Vienna, Austria

and

Vladimir Pronyaev

Institute of Physics and Power Engineering (IPPE)
Obninsk, Russia

May 2015

^{209}Bi(n,f) and ^{nat}Pb(n,f) Cross Sections as a New Reference and Extension of the ^{235}U, ^{238}U and ^{239}Pu(n,f) Standards up to 1 GeV

Benjaminas Marcinkevicius, Stanislav Simakov

IAEA Nuclear Data Section
Vienna, Austria

and

Vladimir Pronyaev
Institute of Physics and Power Engineering (IPPE)
Obninsk, Russia

Abstract

The ^{209}Bi(n,f) and ^{nat}Pb(n,f) reaction cross sections are used as a reference for neutron energies above 30 MeV in the accelerator driven system applications. This report describes the update of the evaluation for ^{209}Bi(n,f) reaction released by the IAEA in 1997 and the new evaluation for ^{nat}Pb(n,f). Additionally, the evaluation of the neutron fission standard cross sections of ^{238}U, ^{235}U and ^{239}Pu were extended above 200 MeV up to 1 GeV. This report summarizes the results of the collection and analysis of available experimental data, CEM and Talys theoretical model calculations, and the evaluation of experimental data by the GMAP code. The final evaluated data for the ^{238}U, ^{235}U, ^{239}Pu, ^{nat}Pb, ^{209}Bi neutron induced fission cross sections are presented in both tabular and parameterization form. These evaluations are presented in the ENDF and text formats as well as NJOY plots and can be downloaded from the IAEA Neutron Reaction Standards web page (www-nds.iaea.org/standards/)

May 2015

TABLE OF CONTENTS

1.   Introduction

The neutron-induced fission cross sections of bismuth and lead at intermediate energies are crucial for the design and operation of accelerator-driven systems. Lead-bismuth eutectic is considered a liquid coolant and target for the spallation sources presently under operation, construction or design [1] as well as for the accelerator driven reactor design [2].

On the other hand, the ^{209}Bi(n,f) and ^{nat}Pb(n,f) reactions were recognised as a convenient reference during the measurement of other cross sections at high energies. The relatively high reaction threshold of 21 MeV eliminates the influence of low energy neutrons. These cross sections are a smooth and gradually increasing function of energy that decreases impact of a typical spectrometer energy resolution. Bi and Pb are chemically nonaggressive and cheap materials which allow easy mechanical processing and sample preparation for the fission chamber.

In 1997 an expert group under the auspices of the Nuclear Data Section of IAEA issued a "secondary standard" – recommended ^{209}Bi(n,f) cross section evaluated from threshold up to 1000 MeV with uncertainties of 50% at neutron energies from 20 to 40 MeV, 13 - 10% from 40 to 160 MeV and about 30% above 169 MeV [3]. This evaluation was based on measurements [4 - 7] published before 1997. It is important to note that the highest energy of cross section measurement at that time was 380 MeV. Since then, several new measurements [8 - 16] have been carried out and published. Consequently, the revisiting of the old evaluation could result in a more accurate reference cross section.

The IAEA Technical Meeting "Toward a New Evaluation of Neutron Standards", held 8 - 12 July 2013, recommended to revisit and eventually update the ^{209}Bi(n,f) evaluation [17]. Considering the results of a comparatively large amount of experiments for the ^{nat}Pb(n,f) reaction we additionally performed an evaluation of this reaction.

To implement this goal the following work has been carried out:
- collection and critical review of the available experimental cross sections for the (n,f) reaction on ^{209}Bi and ^{nat}Pb;
- calculation of ^{209}Bi and ^{nat}Pb (n,f) cross sections employing CEM and Talys codes;
- generation of recommended cross sections for both reactions using the least square method (GMAP code) and up-to-date set of neutron reactions used in the measurements of ^{209}Bi(n,f) and ^{nat}Pb(n,f);
- inclusion of the high energy proton induced fission cross section above 200 MeV to reduce the uncertainties of the reference cross section;
- comparison of the new ^{209}Bi(n,f) and ^{nat}Pb(n,f) evaluations with the main evaluated libraries and relevant theoretical models;
- conversion of the new evaluations to the ENDF-6 formatted files and processing by the NJOY-2012 code;
- update of the GMAP code and supplementary documentation to make it more user friendly.

2.   Experimental Data

Information about all published measurements of the ^{209}Bi(n,f), ^{nat}Pb(n,f) and $^{204-208}$Pb(n,f) reaction cross sections are presented in Table 1, Table 2 as well as Fig. 1 - 4.

The documentation and (n,f) data measured in 1950 the Institute of Nuclear Problems, Moscow [18] and [19] are not available.

These Tables are followed by graphical representation of data and description of experimental data used in the evaluation. Additional information can be found in APPENDIX A: Reaction Cross Section and Ratio Measurements. Plots of the measured cross sections and reaction ratios illustrate the status of available data.

Table 1. Published measurements of the ^{209}Bi(n,f) reaction cross section.

First author and Ref.	Year Lab	Neutron Source	Neutron Energy, MeV	Results of measurements: Cross Section or Ratio	Fission detector, method, normalisation.	EXFOR Entry
E.L. Kelly [20]	1948 Cyclotron, Berkeley, CA	Pb(d,xn), E_d = 81 - 190 MeV	84 25 - 84	^{209}Bi(n,f)/^{232}Th(n,f) (thin Bi) ^{209}Bi(n,f)/^{232}Th(n,f) (thick Bi)	Ionization chamber, relative to ^{232}Th(n,f)	14401.002
V.I. Goldanskiy [4]	1955 Synchrocyclotron, Troitsk	Cu(d,xn) E_d = 280 MeV; ^{9}Be(p,xn)	120 210, 315, 380	^{209}Bi(n,f)	Ionization chamber, relative to ^{12}C(n,2n)	41212.010
P.E. Vorotnikov [5]	1984 KIAE, Moscow	T(d,n)	18, 21.7, 22.6, 23.3	^{209}Bi(n,f)	Glass track detector, relative to ^{19}F(n,2n) and ^{127}I(n,2n)	40844.003
P. Staples [8]	1995, WNR, Los Alamos	W(p,xn) E_p = 800 MeV	30 - 500	^{209}Bi(n,f)/^{235}U(n,f)	Ionization chamber, ToF, relative to ^{235}U	will be included in EXFOR
V.P. Eismont [7]	1996 TSL, Uppsala	^{7}Li(p,n)	45, 73	^{209}Bi(n,f)/^{238}U(n,f) ^{209}Bi(n,f) (derived)	TFBC, ToF, relative to (n,p) and ^{238}U(n,f)	23217.002 23217.003
O. Shcherbakov [9]	2001 GNEIS, Gatchina	Pb(p,xn) E_p = 1 GeV	30 – 196	^{209}Bi(n,f)/^{235}U(n,f) ^{209}Bi(n,f) (derived)	Ionization chamber, ToF, relative to ^{235}U	41455.008 41455.015
A.N. Smirnov [12]	2004 TSL Uppsala	^{7}Li(p,n)	34.5 – 173	^{181}Ta(n,f)/^{209}Bi(n,f) ^{nat}W(n,f)/^{209}Bi(n,f) ^{197}Au(n,f)/^{209}Bi(n,f) ^{nat}Hg(n,f)/^{209}Bi(n,f) ^{205}Tl(n,f)/^{209}Bi(n,f) ^{nat}Pb(n,f)/^{209}Bi(n,f) ^{204}Pb(n,f)/^{209}Bi(n,f) (derived) ^{206}Pb(n,f)/^{209}Bi(n,f) (derived) ^{207}Pb(n,f)/^{209}Bi(n,f) (derived) ^{208}Pb(n,f)/^{209}Bi(n,f) ^{209}Bi(n,f) (derived from ratio) ^{209}Bi(n,f)/^{238}U(n,f)	TFBC (Thin Film Breakdown Counters) and Ionization chambers, ToF, relative to ^{238}U	22882.008 22882.007 22882.006 22882.022 22882.017 22882.004 22882.014 22882.015 22882.016 22882.005 22882.003 22882.002
A.V. Fomichev [13]	2004 GNEIS, Gatchina	Pb(p,xn) E_p = 1 GeV	30 – 414	^{209}Bi(n,f)	Multi-plates ionization chamber, ToF, relative to ^{235}U	41444.004

First author and Ref.	Year Lab	Neutron Source	Neutron Energy, MeV	Results of measurements: Cross Section or Ratio	Fission detector, method, normalisation.	EXFOR Entry
I.V. Ryzhov [14]	2006 TSL Uppsala and Louvain-la-Neuve	^{7}Li(p,n)	34.7 – 174	^{209}Bi(n,f)	Ionization chambers, ToF, relative to ^{238}U(n,f)	22903.008
A.B. Laptev [10]	2007 GNEIS, Gatchina	Pb(p,xn) E_p = 1 GeV	28 – 200	^{209}Bi(n,f)/^{235}U(n,f) ^{209}Bi(n,f) (derived from ratio)	Ionization chambers, ToF, relative to ^{235}U	41487.006 41487.012
R. Nolte [15]	2007 Louvain-la-Neuve, iThemba LABS	^{7}Li(p,n)	33, 45, 60 and 100,150, 200	^{209}Bi(n,f)	Fission Ionization Chamber, ToF, relative to (n,p) or ^{238}U(n,f)	23078.004
D. Tarrio [16]	2011 CERN	Pb(p,xn) P_p = 20 GeV/c	43.7 – 1000	^{nat}Pb(n,f)/^{209}Bi(n,f) ^{209}Bi(n,f) (derived from ratio) ^{209}Bi(n,f)/^{235}U(n,f) ^{209}Bi(n,f)/^{238}U(n,f)	PPAC (parallel plate avalanche counter), relative to ^{238}U and ^{235}U	23151.006 23151.008 23151.004 23151.005

Table 2. Published measurements of the ^{nat}Pb(n,f) and $^{204-208}$Pb(n,f) reaction cross section and cross section ratio.

First author and Ref	Year and Lab	Neutron Source	Neutron Energy, MeV	Results of Measurements: Cross Section or Ratio	Fission detector, method, normalisation.	EXFOR Entry
E.L. Kelly [20]	1948 Cyclotron, Berkeley, CA	Pb(d,xn), E_d = 81 -190 MeV	84 25 – 84	^{nat}Pb(n,f)/^{232}Th(n,f) (thin Pb) ^{206}Pb(n,f)/^{232}Th(n,f) (thin Pb) ^{207}Pb(n,f)/^{232}Th(n,f) (thin Pb) ^{208}Pb(n,f)/^{232}Th(n,f) (thin Pb) ^{nat}Pb(n,f)/^{232}Th(n,f) (thick Pb)	Ionization chamber, relative to ^{232}Th(n,f)	14401.003
V.I. Goldanskiy [4]	1955 Synchrocyclotron, Troitsk	Cu(d,xn) E_d = 280 MeV; ^{9}Be(p,xn)	120, 210, 315, 380	^{nat}Pb(n,f)	Ionization chamber	41212.009
P.E. Vorotnikov [5]	1984 KIAE, Moscow	T(d,n)	18, 21.7, 22.6, 23.3	^{nat}Pb(n,f)	Glass track detector, relative to ^{19}F(n,2n), ^{127}I(n,2n)	40844.002
P. Staples [8]	1995, WNR, Los Alamos	W(p,xn) E_p = 800 MeV	30 - 500	^{nat}Pb(n,f)/^{235}U(n,f)	Ionization chamber, ToF, relative to ^{235}U	will be included in EXFOR
O. Shcherbakov [9]	2001 GNEIS, Gatchina	Pb(p,xn) E_p = 1 GeV	30 – 196	^{nat}Pb(n,f)/^{235}U(n,f) ^{nat}Pb(n,f) (derived)	Ionization chamber, ToF	41455.007 41455.014
A.N. Smirnov [12]	2004, TSL Uppsala	^{7}Li(p,n)	34.5 – 173	^{nat}Pb(n,f) (derived) ^{204}Pb(n,f) (derived) ^{206}Pb(n,f) (derived) ^{207}Pb(n,f) (derived) ^{208}Pb(n,f) (derived) ^{204}Pb(n,f)/^{209}Bi(n,f) (derived) ^{206}Pb(n,f)/^{209}Bi(n,f) (derived) ^{207}Pb(n,f)/^{209}Bi(n,f) (derived) ^{208}Pb(n,f)/^{209}Bi(n,f) ^{nat}Pb(n,f)/^{209}Bi(n,f)	Thin Film Breakdown Counters (TFBC) and Frisch –gridded ionization chambers, ToF and Unfolding, relative to ^{238}U(n,f)	22882.009 22882.018 22882.019 22882.020 22882.010 22882.014 22882.015 22882.016 22882.005 22882.004
I.V. Ryzhov [14]	2006 TSL Uppsala, LLN, Louvain-la-Neuve	^{7}Li(p,n)	34.7 – 174	^{nat}Pb(n,f) (derived) ^{204}Pb(n,f) ^{206}Pb(n,f) ^{207}Pb(n,f) ^{208}Pb(n,f)	Frisch-gridded Ionization Chamber, ToF, relative to ^{238}U(n,f)	22903.007 22903.003 22903.004 22903.005 22903.006

First author and Ref	Year and Lab	Neutron Source	Neutron Energy, MeV	Results of Measurements: Cross Section or Ratio	Fission detector, method, normalisation.	EXFOR Entry
R. Nolte [15]	2007 Louvain-la-Neuve, iThemba LABS	^{7}Li(p,n)	33, 45, 60 and 100,150, 200	^{nat}Pb(n,f)	Fission Ionization Chamber, ToF, relative to (n,p) or ^{238}U(n,f)	23078.005
D. Tarrio [16]	2011 CERN	Pb(p,xn) P_p = 20 GeV/c	43.7 – 1000	^{nat}Pb(n,f) (derived from ratio) ^{nat}Pb(n,f)/^{209}Bi(n,f) ^{nat}Pb(n,f)/^{235}U(n,f) ^{nat}Pb(n,f)/^{238}U(n,f)	PPAC, relative to ^{238}U and ^{235}U	23151.007 23151.006 23151.002 23151.003

Fig. 1. ^{nat}Pb(n,f) cross section up to 300 MeV: comparison of the neutron induced fission measurements with evaluation ENDF/HE-VI based on [21] for ^{208}Pb(n,f), JENDL/HE [22] and the latest parameterization [16] (dashed line).
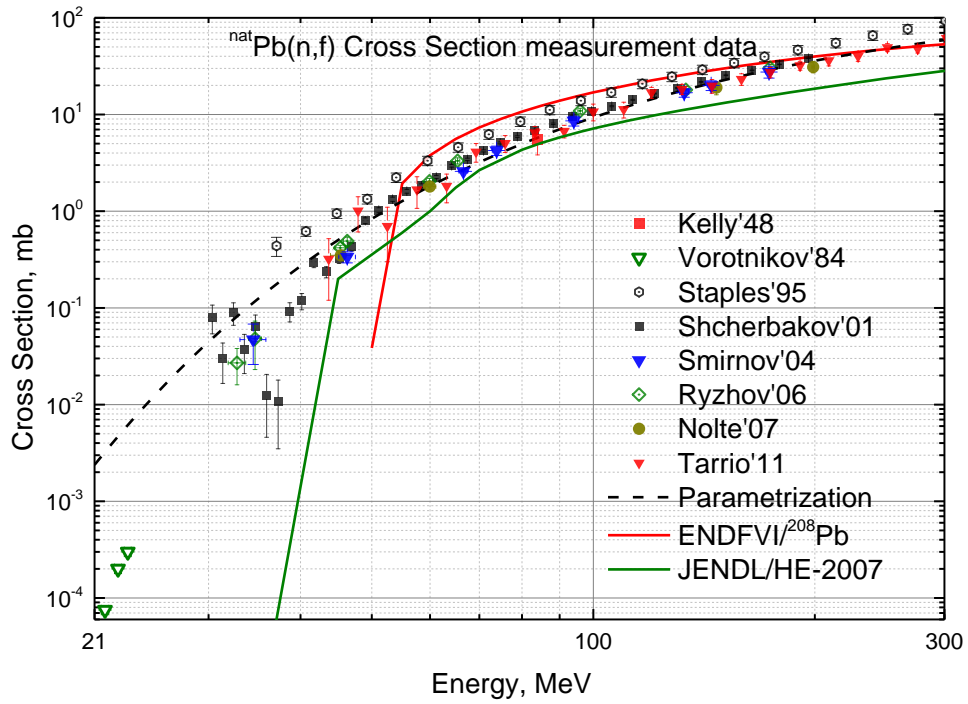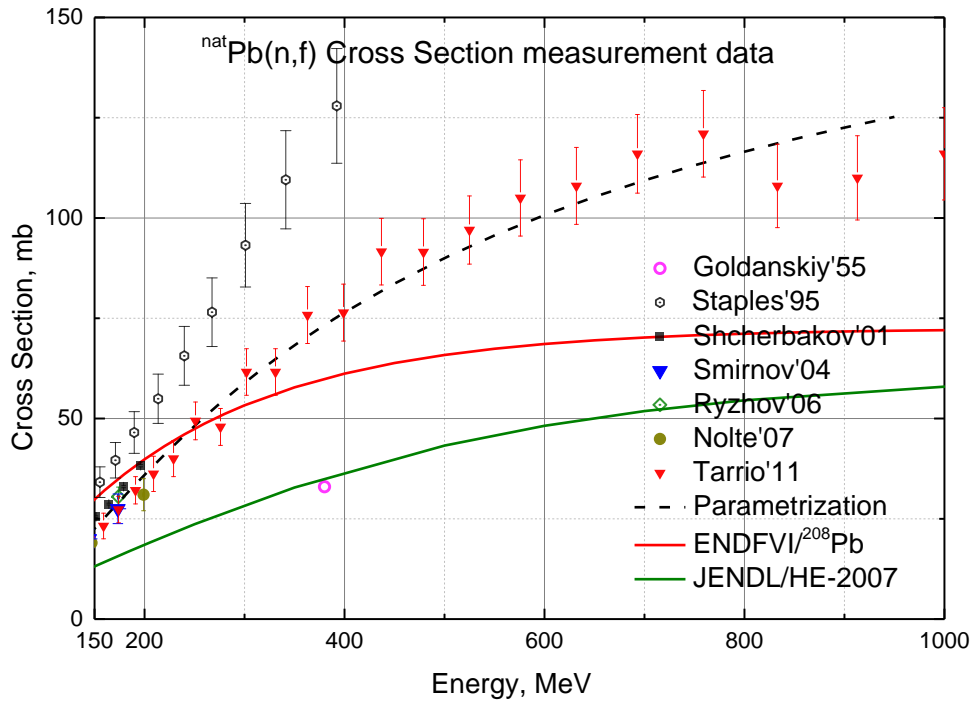

Fig. 2. ^{nat}Pb(n,f) cross section from 150 up to 1000 MeV: comparison of the neutron induced fission measurements with evaluation ENDF/HE-VI based on [21] for ^{208}Pb(n,f), JENDL/HE-2007 [22] and the latest parameterization [16] (dashed line).

Fig. 3. ^{209}Bi(n,f) cross section up to 100 MeV: comparison of neutron induced fission measurements with the IAEA [3], JENDL/HE [22] and ENDF/HE-VI based on [21] evaluations.

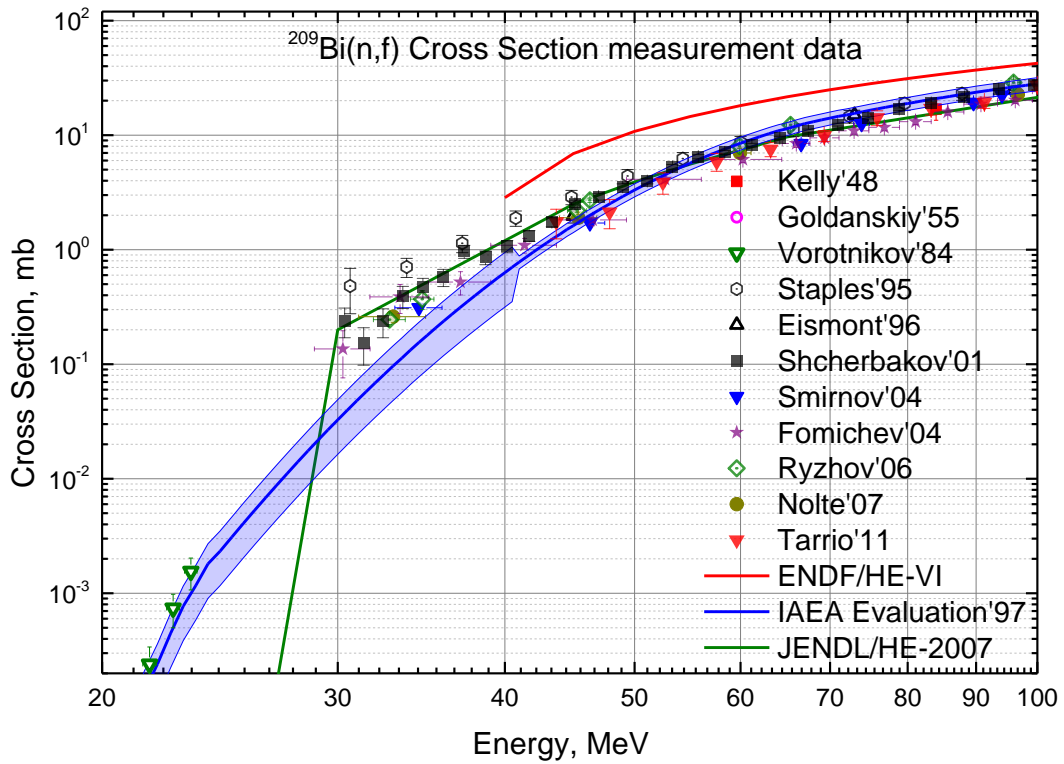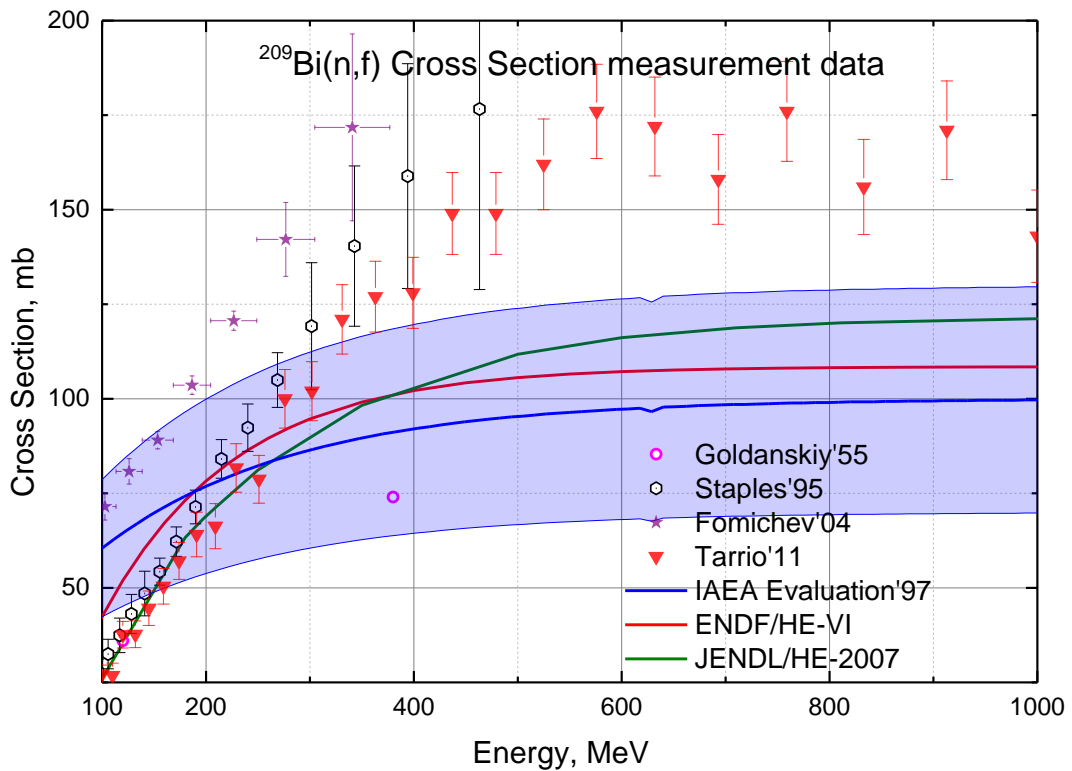Fig. 4. ^{209}Bi(n,f) cross section from 150 up to 1000 MeV: comparison of neutron induced fission measuremnts with the IAEA [3], JENDL/HE [22] and ENDF/HE-VI based on [21] evaluations.

2.1. Measurements by E.L. Kelly et al.

Kelly's data are the oldest (1948) available where he measured neutron induced fission in the energy range 25 to 84 MeV using thin and thick lead target as neutron source at the Berkley cyclorton, CA [20]. The neutron source had energy spread at FWHM of at least 13 MeV. The measurements were carried out with thick and thin targets relative to ^{232}Th fission. The authors reported that there is a significant fission fragment stopping in the samples. Due to the essential energy spread and usage of thick targets the data was not included in evaluation. It was noticed that Kelly's data deviates significantly from other experiments at lower neutron energies.

The absolute (n,f) cross sections for ^{nat}Pb and ^{209}Bi were derived from the original author's data for comparison and a consistency check with other experimental data and evaluations. For this purpose the newest ^{232}Th(n,f) evaluation above 60 MeV from ROSFOND-2010 [23] was used as reference cross section to calculate the absolute cross sections presented in Table 3.

Table 3. Absolute cross section values derived from ratio measurements at 84 MeV in [20].

Reaction	Cross sections derived from [20], mb	Evaluation, mb
^{nat}Pb(n,f)	5.46	5.76 [16]
^{209}Bi(n,f)	18.96	20.90 ± 2.72 [3]

2.2. Measurements by V.I. Goldanskiy et al.

Goldanskiy's data were measured in 1955 relative to ^{12}C(n,2n) as a flux monitor [4]. The authors used the following reference values for ^{12}C(n,2n): 22 mb at 120 MeV and 21 mb at 380 MeV.

Since then the ^{12}C(n,2n) cross section was re-evaluated that should be taken into account. We used the values from the JENDL/HE-2007 evaluation [22]: 23 mb at 120 MeV and 20 mb at 380 MeV. E. Kim et al. [24] measured ^{12}C(n,2n) cross section up to 147 MeV, the value derived from his results equals 25 ± 8.35 mb at 120 MeV, which agrees with JENDL/HE-2007.

Finally Goldanskiy's cross section at 120 MeV was included in the evaluation of the ^{209}Bi(n,f) cross section using the JENDL/HE-2007 cross section as a reference, however an additional uncertainty of 30% was assigned to his point.

At 380 MeV Goldanskiy's cross section of ^{209}Bi(n,f) is significantly lower than all known measurements (see Fig. 3). Since the same normalisation method was applied for the ^{nat}Pb(n,f) measurements, the fission cross sections at 380 MeV for both targets ^{nat}Pb and ^{209}Bi were excluded from the present evaluation.

2.3. Measurements by P.E. Vorotnikov et al.

In this experiment the ^{209}Bi(n,f) and ^{nat}Pb(n,f) cross sections were measured at 18.0, 21.7, 22.6 and 23.3 MeV by counting the fragment tracks in glass detectors [5]. The incident neutron flux was measured by threshold activation reactions ^{19}F(n,2n) and ^{127}I(n,2n), while reference cross sections were taken from [25].

For the ^{nat}Pb(n,f) reaction the authors only gave the upper limit for the cross section value and total uncertainties. For ^{209}Bi(n,f) only the energy uncertainties are provided.

These data were not included in the GMAP evaluation as there are too few points in this energy region, moreover the cross section has steep energy slope.

2.4. Measurements by P. Staples et al.

The neutron-induced fission cross section ratios from threshold up to 500 MeV for ^{nat}Pb and ^{209}Bi have been measured relative to ^{235}U at the WNR white neutron source at Los Alamos Lab [8]. A white spectrum of neutrons was produced by 800 MeV protons. The fission reaction rate was determined using a fast parallel plate ionization chambers and time-of-flight technique.

Data was digitized from figures provided by P. Staples. It was reported that there were two foils of ^{nat}Pb and ^{209}Bi, thus we decided to add four datasets obtained with the different foils in the evaluation. The uncertainties include: digitized statistics (4 - 25%), sample mass uncertainty (10%), uncertainty due to flight path (0.3%), wrap around due to beam cycle (0.1%), attenuation of the beam (0.7%), charged particle contribution (0.5%) and total monitor uncertainty (5%). Sample mass, flight path and monitor uncertainties were treated as fully correlated through all energy ranges where possible. Energy uncertainties were also reported: due to flight path uncertainty (0.1%) and calibration (0.1%).

At low neutron energies we increased the uncertainties of the cross section because the values were discrepant with other experiments (see Fig. 1). The discrepancy was extremely significant for the ^{nat}Pb cross section ratio. The ^{209}Bi(n,f)/^{235}U(n,f) data was treated as an absolute ratio, while ^{nat}Pb(n,f)/^{235}U(n,f) - as shape ratio.

The author recommended to use experimental data with caution as data analysis was not fully completed. This was taken into account and uncertainties were increased in all energy ranges. Data was compiled in EXFOR.

2.5.   Measurements by V.P. Eismont et al.

The measured ^{209}Bi(n,f)/^{238}U(n,f) ratios at 45 and 73 MeV [7] were included in our analysis. The authors provided total uncertainty and its components: statistical uncertainty 7%, mass of targets 0.5%, target thickness correction 0.5%, TOF spectrum decomposition < 8%, energy spectrum extrapolation < 7%, linear momentum transfer correction 0.5%.

We treated the mass and thickness uncertainties as fully correlated through all energy ranges, others as uncorrelated.

2.6.   Measurements by O.A. Shcherbakov et al.

Two datasets measured by Shcherbakov et al. were used in our evaluation: ^{nat}Pb(n,f)/^{235}U(n,f) and ^{209}Bi(n,f)/^{235}U(n,f) up to 196 MeV. The authors have provided statistical and systematic energy dependant uncertainties as well as energy resolution. Reported uncertainties are due to: separation of fission and background events in pulse-height spectra (< 0.5%); energy-independent neutron background (< 0.015%); energy-dependent neutron background (< 1.5%); correction of neutron beam attenuation for different target foils (0.8%); correction for anisotropy and linear momentum transfer (max 1%); fission cross-section ratio normalization due to the calculation of the targets thickness and fission fragments detection efficiency (2%); maximal admixtures of impurities in Pb targets (0.1 − 5%);

Uncertainties of maximal admixtures in the Pb and Bi targets and normalization of the fission cross-section ratio were treated as fully correlated uncertainties, since we assumed that only one determination of the sample thickness and impurities was made. However, because the influence of these factors varies from 0.1 to 5% and depends on the energy range, it was decided that the data would be split into three separate correlated data sets.

It was noticed that cross-section values at two energies 35.98 MeV and 37.30 MeV for ^{nat}Pb(n,f) are significantly lower than the overall trend - they were removed from the evaluation (see Fig. 1).

2.7.   Measurements by A.V. Fomichev et al.

This experiment was performed at the GNEIS facility in Gatchina and published in [11, 13]. The ^{209}Bi(n,f) cross section was measured relative to the ^{235}U(n,f) cross section up to 414 MeV.

However, only the absolute ^{209}Bi(n,f) cross section was published by the authors and compiled in the EXFOR Entry 41444.004. For the conversion to absolute values the authors used the recommended ^{235}U(n,f) cross section from Standards issued by the IAEA in 1997 [3] where this cross section is given as numerical data and parameterisation only up to 200 MeV. We assumed that ^{235}U(n,f) reference cross section was extrapolated above the 200 MeV using the same parameterization and calculated the ^{235}U(n,f)/^{209}Bi(n,f) ratio to use it in our evaluation.

The data published by Fomichev are from the same experiment as A.B. Laptev et al.'s [10], however the data reduction process was different. Hence we decided that Fomichev' data will be used for the energies unavailable in Laptev' publication [10].

Uncertainties reported and included in our evaluation comprise: statistics, fully correlated measurement of the sample mass (2%), energy dependant systematic error (< 14%) and energy resolution.

2.8. Measurements by A.N. Smirnov et al.

These measurements were carried out several times in The Svedberg Laboratory (TSL), Uppsala, in collaboration with the V.G. Khlopin Radium Institute, St. Petersburg [6, 12].

Two data sets were used in our evaluation: the $^{nat}Pb(n,f)/^{209}Bi(n,f)$ and $^{209}Bi(n,f)/^{238}U(n,f)$ ratios in the energy range from 34.5 to 173.3 MeV. They were taken from the latest publication [12], which superseded the previous and preliminary one [7].

The uncertainties were analysed and reported by the authors. Our evaluation includes the uncertainties of the total cross section (excluding detector efficiency) and energy. In addition to the total uncertainty we included those related to the calculation of relative detection efficiency (5%, fully correlated) and variation of the detection efficiency from one sandwich to another in mosaic arrangement (0.6%).

2.9. Measurements by I.V. Ryzhov

The measurements of fission cross sections for ^{209}Bi and separated isotopes $^{204,206,207,208}Pb$ were performed using the neutron sources of the Louvain-la-Neuve (LLN) at energies 33, 45 and 60 MeV and The Svedberg Laboratory (TSL), Uppsala in the energy range from 35 to 180 MeV [14]. The fission cross section for ^{nat}Pb was derived by the authors from isotopes cross sections.

The cross sections were measured relative to $^{238}U(n,f)$ and converted to the absolute cross sections using the IAEA standard [3]. At 60 MeV the neutron fluence has been simultaneously determined by the main fission detector and a fission chamber monitor calibrated relative to a proton recoil telescope. The results of the inter-comparison were found to be consistent within 3%.

The $^{nat}Pb(n,f)$ and $^{209}Bi(n,f)$ data published by the authors and compiled in EXFOR are absolute cross sections - we also used them in the same form in our evaluation. The data measured at LLN and TSL were included in our evaluation as two datasets, since the most of the uncertainty components do not correlate. Authors provided the energy resolution, statistical and mass uncertainties (2%). Since the same ionization chamber was used the sample mass uncertainties were treated as fully correlated between the datasets.

2.10. Measurements by R. Nolte

The fission cross sections were measured at energies ≈ 35, 45 and 60 MeV at the neutron beam facility of the Université Catholique de Louvain (UCL) in Louvain-la-Neuve and at energies ≈ 100, 150 and 200 MeV in the iThemba Laboratory for Accelerator Based Sciences (TLABS) in Cape Town [15]. The incident neutron peak fluence was measured by recoil proton telescopes, i.e. the $^{nat}Pb(n,f)$ and $^{209}Bi(n,f)$ cross sections were obtained relative to the differential n-p scattering derived from [26].

These datasets were added to our evaluation as absolute cross sections. Authors reported the energy resolution, neutron energy uncertainty, the total cross section uncertainty (without monitor uncertainty) and monitor uncertainty (max 5%).

Additionally the systematic and statistical uncertainty components, which contribute to the total uncertainty, were provided. They were subtracted from total uncertainty and used as a separate input of systematic uncertainty for the GMAP code. Subtracted uncertainties include: chamber efficiency (1.6%), monitor reading (2%), neutron transport in fission transfer (0.7%), loss of events due to pulse height threshold (0.9%), dead time losses (0.4%), distance between RPT and PPFC position (0.2%), neutron absorption in air (0.3%) and spatial inhomogeneity of the neutron fluence (1.3%). Other provided uncertainties depend on neutron energy, it was not possible to subtract them from the total uncertainty. Loss of events due to the pulse height threshold was treated as fully correlated uncertainty in all energy ranges.

2.11. Measurements by A.B. Laptev

The $^{209}Bi(n,f)/^{235}U(n,f)$ cross section ratio measured in [10] was used in our evaluation as absolute ratio. The authors provided statistical and systematic energy dependant uncertainties as well as energy resolution.

Reported systematic uncertainties result from: separation of the fission and background events in the pulse-height spectra ($< 0.5\%$); energy-independent neutron background ($< 0.015\%$); energy-dependent neutron background ($< 1.5\%$); correction for the neutron beam attenuation in the different target foils (0.8%); correction for anisotropy and linear momentum transfer (max 1%); fission cross-section ratio normalization due to the calculation of the targets thickness and fission fragments detection efficiency (2%); maximal admixtures of impurities in the Bi targets (0.1-5%).

Uncertainties of maximal admixtures in the Bi targets and normalization of the fission cross-section ratio were treated as fully correlated uncertainties, since we supposed that only one measurement of the sample thickness and impurities was made. However, because the influence of these factors varies from 0.1 to 5% and depends on the energy, the data was split into three separate data sets.

2.12.   *Measurements by D. Tarrio*

The cross sections were measured for ^{nat}Pb and ^{209}Bi (n,f) reactions from 43.7 to 1000 MeV at the CERN Time-of-Flight (n_TOF) facility [16]. The cross sections were measured relative to ^{238}U(n,f) and ^{235}U(n,f).

The summary of Tarrio's data and how the uncertainties were treated in our evaluation are summarized in Table 4.

Table 4. CERN n_ToF data and analysis of uncertainties for use in the GMAP fit.

Reactions Ratio	Analysis of Data Uncertainties
^{nat}Pb(n,f)/^{209}Bi(n,f), ^{209}Bi(n,f)/^{235}U(n,f), ^{nat}Pb(n,f)/^{235}U(n,f)	Statistical and systematic uncertainties were provided by authors. Systematic uncertainties are: sample mass (1.2%), beam spot size (2.5%), sample thickness and threshold error (3.5%), energy dependant error due to anisotropy (max 2%). Sample mass, beam spot size and sample thickness uncertainties were treated in our evaluation as fully correlated in the whole energy range as well as correlated between different data sets.
^{209}Bi(n,f)/^{238}U(n,f), ^{nat}Pb(n,f)/^{238}U(n,f)	The same as above, except that the fully correlated uncertainty for the shape ratio can not be specified for GMAP.

Since the authors measured the ^{nat}Pb(n,f) and ^{209}Bi(n,f) cross sections relative to ^{238}U(n,f) and ^{235}U(n,f), we compared the ^{238}U/^{235}U(n,f) ratio derived from their measurements with the ratio of the standards [27], Fig. 5. We assume that the observed systematic difference of 7-8% results from the ^{238}U(n,f) measurements. As Fig. 6 shows, the ^{209}Bi(n,f) cross section derived from ^{209}Bi(n,f)/^{235}U(n,f) matches the evaluated ^{209}Bi(n,f) cross section while derived from ^{209}Bi(n,f)/^{238}U(n,f) is systematically lower.
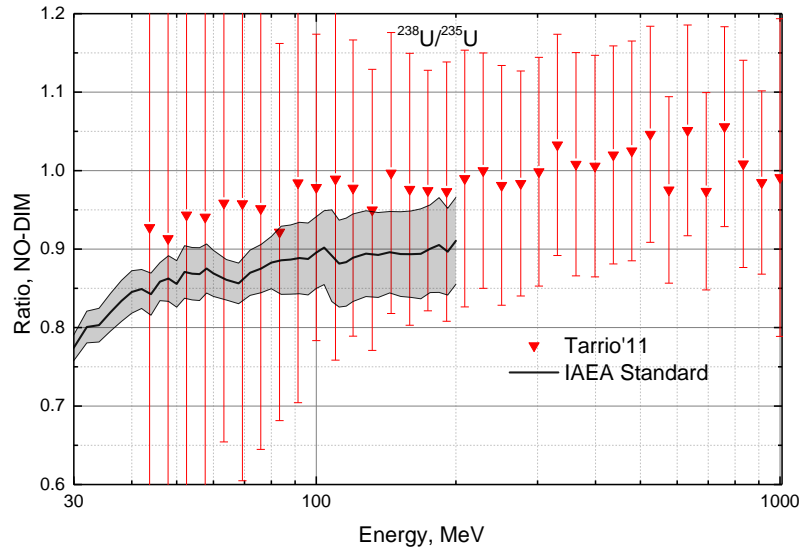
Fig. 5. Comparison of ^{238}U/^{235}U (n,f) ratio obtained from D. Tarrio's experiment [16] with the IAEA Standards [27]. The plotted uncertainty bars of Tarrio'11 data reflect the statistical uncertainty component of the measured ^{209}Bi(n,f)/^{238}U(n,f) ratio.

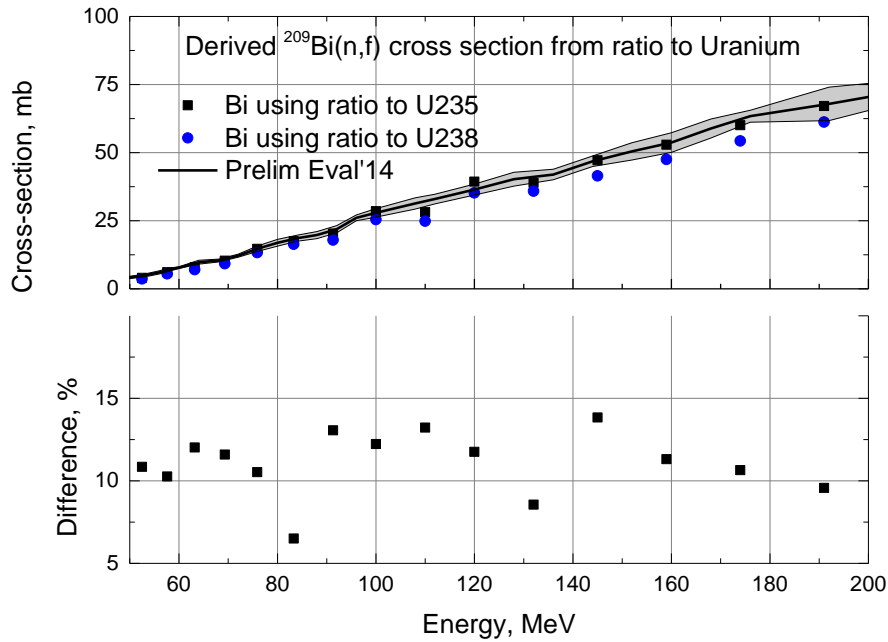Fig. 6. Comparison of the ^{209}Bi(n,f) cross sections calculated from ratios ^{209}Bi(n,f)/^{238}U(n,f) and ^{209}Bi(n,f)/^{235}U(n,f) and preliminary evaluation: absolute cross sections (top), the difference between ^{209}Bi(n,f) cross sections derived from ratios (bottom). In the preliminary evaluation of ^{209}Bi(n,f) all Tarrio's data was treated as a shape.

3. Theoretical calculations

The GMAP code requires an *a priori* cross section to be defined before running the code. We investigated the possibility to model the (n,f) reaction for lead and bismuth. For this we used the Cascade-Exciton Model (CEM) embedded in the Monte-Carlo code MCNP6 [28] for intermediate and high energy fission, and TALYS [29] for intermediate energies.

3.1. CEM03.03 model calculations

The latest version of the model, CEM03.03, developed by S. Mashnik et al. [30] is available as a stand-alone code CEM03.03 or an optional model in MCNP6. We perform calculations for both ^{209}Bi(n,f) and ^{nat}Pb(n,f) reactions using an option GENX in MCNP6. The comparison of results for ^{nat}Pb(n,f) with other evaluations is displayed in Fig. 7. It can be seen that CEM essentially underestimates the cross sections below 300 MeV, the same holds for ^{209}Bi(n,f).
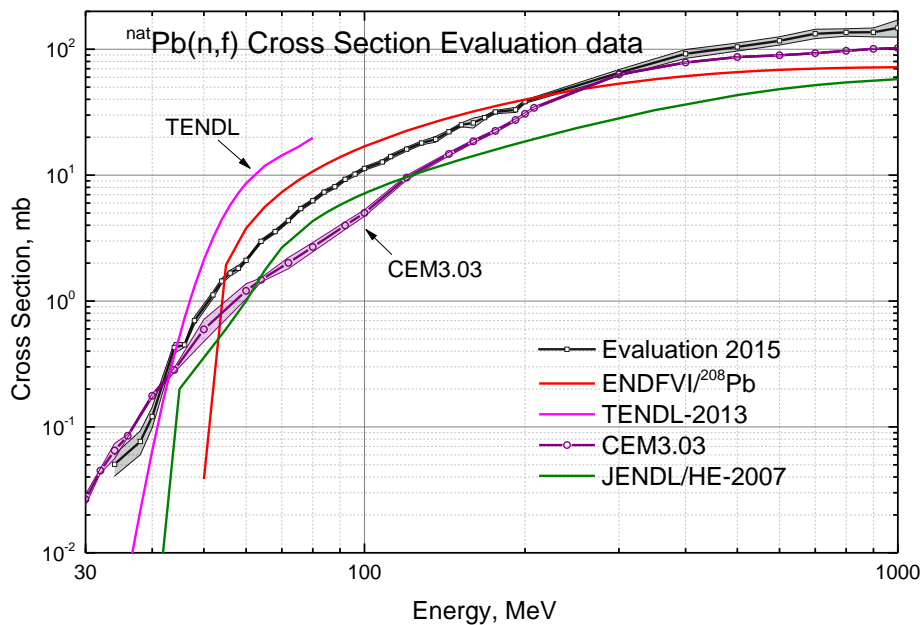

Fig. 7. The ^{nat}Pb(n,f) cross section: comparison between the CEM theoretical calculations and evaluations including our (Evaluation 2015).

3.2. TENDL-2013

The TENDL-2013 evaluation, based on the Tally model, was initially considered as a smooth *a priori* cross section in our evaluation at low energies between 30 – 50 MeV. However, as shown in Fig. 7 for ^{nat}Pb(n,f), the slope and absolute value of the TENDL cross section does not reproduce the current evaluation well. The same tendency was observed for the ^{209}Bi(n,f) reaction. Therefore, the TENDL evaluation was disregarded.

3.3. TALYS

The fission reaction cross section calculations were carried out using TALYS1.6 [29] by varying the different model parameters. Finally, we achieved the best fit which was used as an *a priori* cross section in the GMA input (see Fig. 8).

The fission barrier was considered as single humped using the rotating finite range model. The excited level densities were represented by the Fermi gas model with adjusted asymptotic level density parameters $\tilde{a}$ and γ, the latter affecting the energy dependence of level density parameter. Although the calculated cross section shape and absolute value are comparable to experimental data, the selected model parameters do not correspond well to the recommendations given in the literature [31].
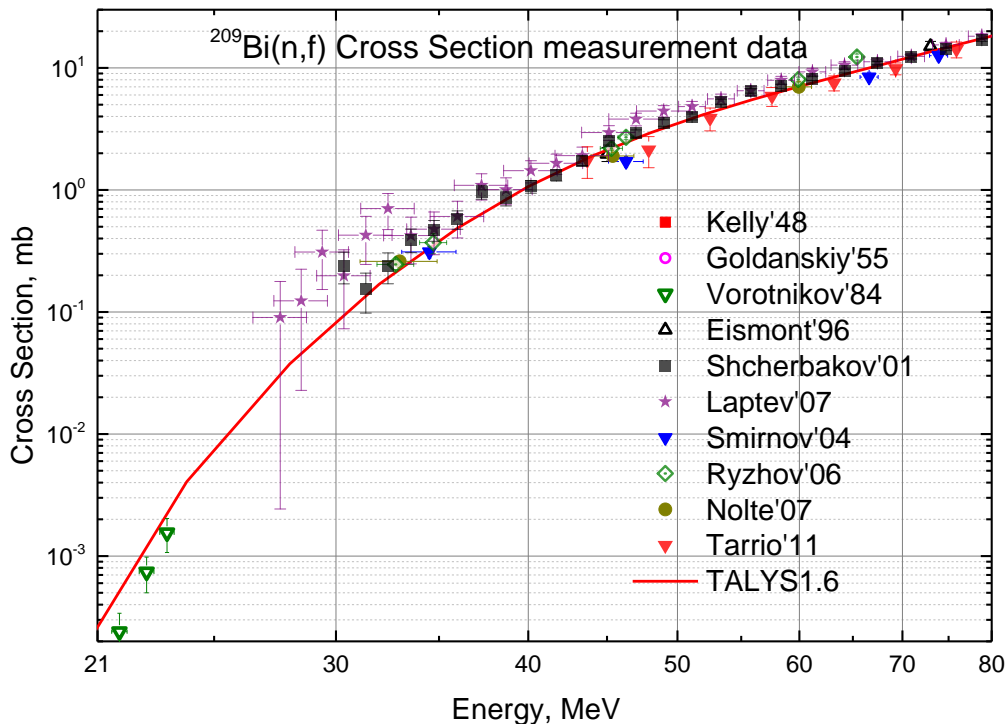
Fig. 8. Comparison of the optimal TALYS calculation with experimental data. Parameters: level density from Fermi model with $\tilde{a}$ = 21.630 1/MeV; γ = 0.047, single humped fission barrier.

4.   Cross Section Evaluation

The GMAP code requires *a priori* cross section values to be provided for the defined energy nodes. An IAEA reference evaluation of [209]Bi(n,f) [3] was selected as an *a priori* for the first iteration. For [nat]Pb(n,f) the parameterization [16] (see Fig. 1) was selected as the best option for the first iteration. Later in the evaluation iteration process, the a priori values were changed to the parameterization carried out in this work. The only exception being the [209]Bi(n,f) reaction cross section below 80 MeV, for which TALYS-1.6 code results were used as an *a priori*.

At energies below 34 MeV, experimental cross section data are inconsistent, rather sparse and pose difficulties being fitted by the GMAP code, resulting in high fluctuations. It was decided to start the GMAP evaluation at 34 MeV. This cut is reasonable since at lower neutron energies the fission cross section is too small (< 0.5 mb) to be realistically applied.

Moreover, we separated an evaluation of the reference [209]Bi and [nat]Pb fission cross sections from other standards evaluation. Inclusion of more reactions into standards GMAP input is not possible without modifying the GMAP code. In addition, replacement of a few reactions within the "standards set" might influence the cross section shape of the standard reactions which should be avoided.

The following cross sections were evaluated simultaneously: [238]U(n,f), [239]Pu(n,f), [235]U(n,f), [nat]Pb(n,f) and [209]Bi(n,f). The cross sections of [238]U(n,f), [239]Pu(n,f), [238]U(n,f) reactions were included into the evaluation as pseudo-experimental cross section data. Pseudo-experimental cross section data were created using GMAP standards input excluding the data sets above 200 MeV. The cross sections of [nat]Pb(n,f) and [209]Bi(n,f), their ratios and ratios to [238]U(n,f) and [235]U(n,f) as well as recent measurements of [238]U/[235]U(n,f) [32] were included in our evaluation.

In our evaluation, the energy bins up to 200 MeV were taken from the standards evaluation. However, the energy bins above 200 MeV were 100 MeV widths to include more experimental points within the bins. We

20

argue that this approach is reasonable, since the fission cross section above the 200 MeV does not vary significantly, moreover the final cross section becomes smoother.

Since ^{238}U(n,f), ^{239}Pu(n,f), ^{238}U(n,f) pseudo experimental data were selected from the standards, we also use the energy-energy correlation matrix in our evaluation (see Fig. 9). The correlation between different cross sections such as ^{238}U(n,f) and ^{235}U(n,f) are insignificant and were neglected in our evaluation.
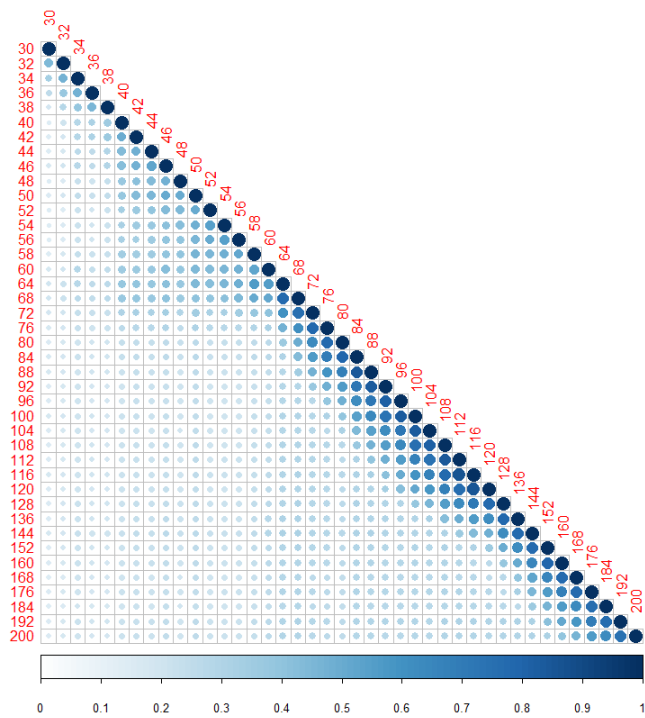

Fig. 9. The energy-energy correlation matrix of ^{238}U(n,f) cross section used in GMAP input for energies from 30 to 200 MeV.

After preliminary evaluation of the ^{nat}Pb(n,f) and ^{209}Bi(n,f) cross sections, it was noticed that evaluated cross section values at some pre-defined energy nodes were uninformative due to the lack of experimental data in the vicinity of these energies. These points were excluded from the final evaluation.

The fact that all known measurements above 200 MeV are relative creates an additional problem. The lack of the measured absolute cross section data above 200 MeV results in an high evaluated cross section uncertainty ($\approx 30\%$), rendering the cross section unsuitable to be used as a reference.

To improve the reference neutron fission cross section uncertainties above 200 MeV, we decided to include proton induced fission data into the evaluation. Newest available ^{238}U(p,f) data was measured by Kotov et al. [33] (see Fig. 10). Including proton induced absolute cross section data improves the cross section uncertainties significantly. This is reasonable at high incident energies since the proton and neutron fission cross section differences are small in comparison with the evaluated uncertainties. The difference between ^{238}U(p,f) and ^{238}U(n,f) cross sections was calculated using the code CEM03.03 and used to scale down the absolute (p,f) cross section. The proton induced fission data on lead or bismuth could also be used. However the fission model predictions as well as experiments are more accurate for actinides than for sub-actinides.

21

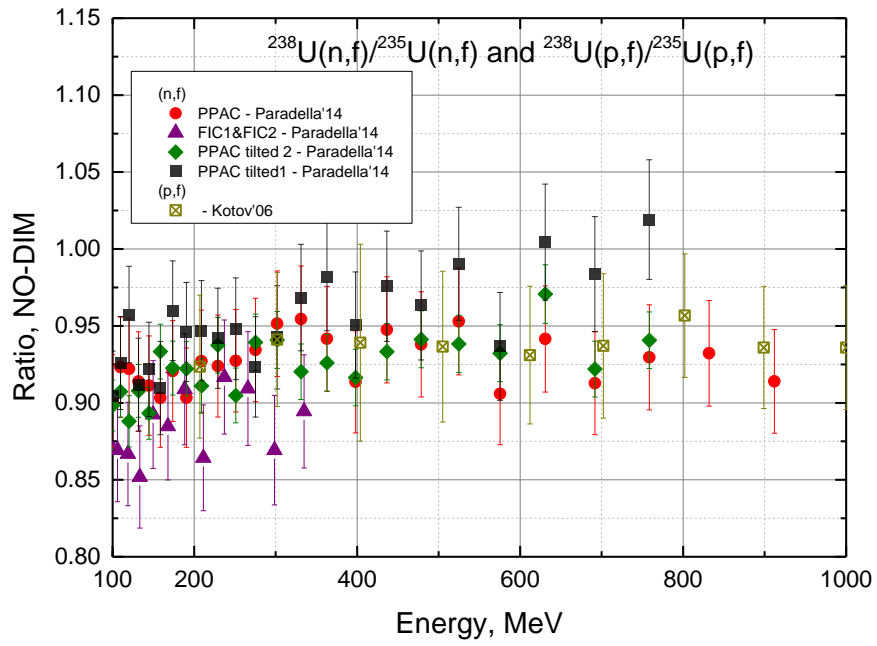Fig. 10. Comparison of recently measured ^{238}U and ^{235}U proton and neutron induced fission data at the intermediate energy: the ^{238}U/^{235}U cross sections ratios for proton and neutron induced fission coincide within uncertainties.

5. Results and Discussions

The current evaluation provides data for the ^{nat}Pb(n,f), ^{209}Bi(n,f), ^{235}U(n,f) and ^{238}U(n,f) cross sections up to 1 GeV. Since there are no new measurements of the ^{239}Pu(n,f) cross section, the evaluation was done only up to 300 MeV with no significant improvement.

The current evaluation's results for standard reactions are compared with the previous standards in Fig. 11. The ^{238}U(n,f) results match within uncertainties. The new ^{235}U(n,f) cross section is systemically lower than the existing standard above 120 MeV, however the difference is small and lies within the uncertainties.
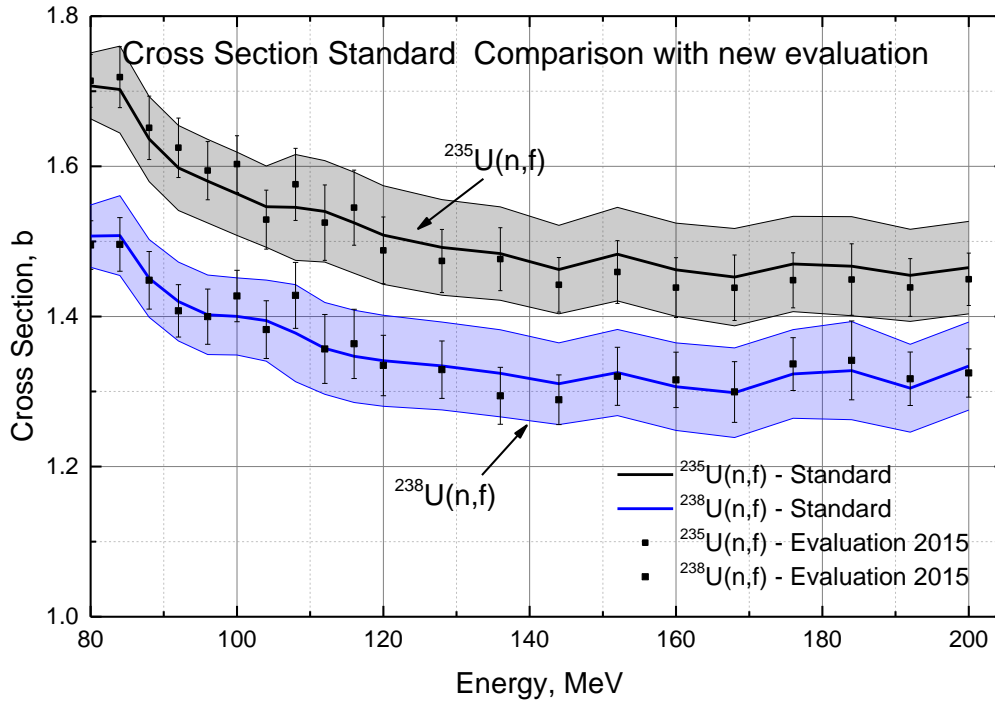

Fig. 11.   Comparison of the ^{235}U(n,f) and ^{238}U(n,f) cross section evaluations with existing standards [27]. *Evaluation 2015* is a new evaluation up to 1 GeV produced together with ^{209}Bi(n,f) and ^{nat}Pb(n,f).

The estimated uncertainties of the new ^{nat}Pb and ^{209}Bi fission cross section evaluation are: < 21% from 34 to 44 MeV; < 10% from 46 to 900 MeV; < 16% at 1 GeV.

APPENDIX B: Reaction Cross Section Evaluation and Parameterization provides more details about the uncertainties, tabulated evaluated reference data and suggested parameterization.

The new evaluations were converted into the ENDF-6 formatted files and processed by the NJOY 2012 code. The files are available for download on the IAEA Neutron Reaction Standards web page (www-nds.iaea.org/standards/) (and additionally as text and plots).

Our analysis indicates that the new absolute measurements of the neutron induced fission cross sections (e.g. relative to n-p scattering) on uranium, bismuth, lead and plutonium have the highest priority in establishing neutron induced fission reaction standards above 200 MeV.

APPENDIX A: Reaction Cross Section and Ratio Measurements

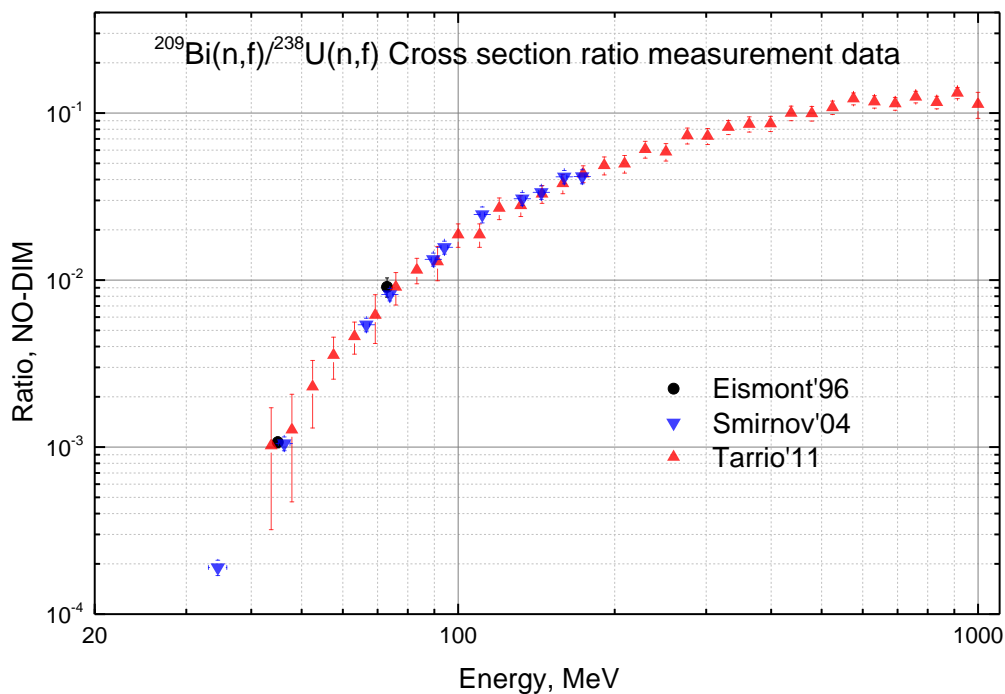Fig. 12. Comparison of measured ^{209}Bi/^{238}U(n,f) cross section ratio data.

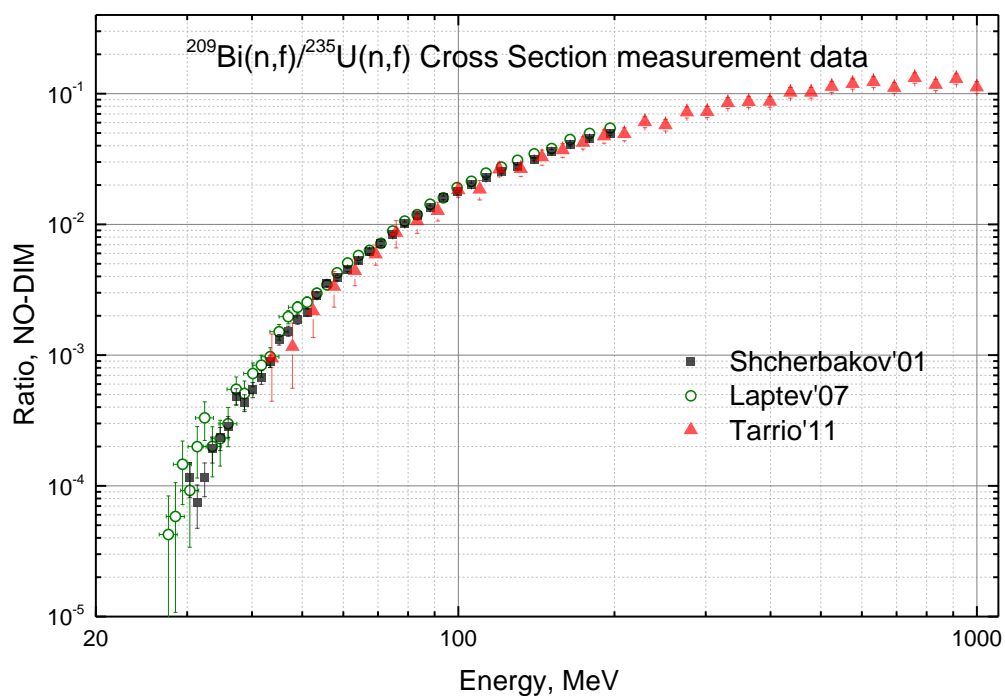Fig. 13. Comparison of measured ^{209}Bi/^{235}U(n,f) cross section ratio data.
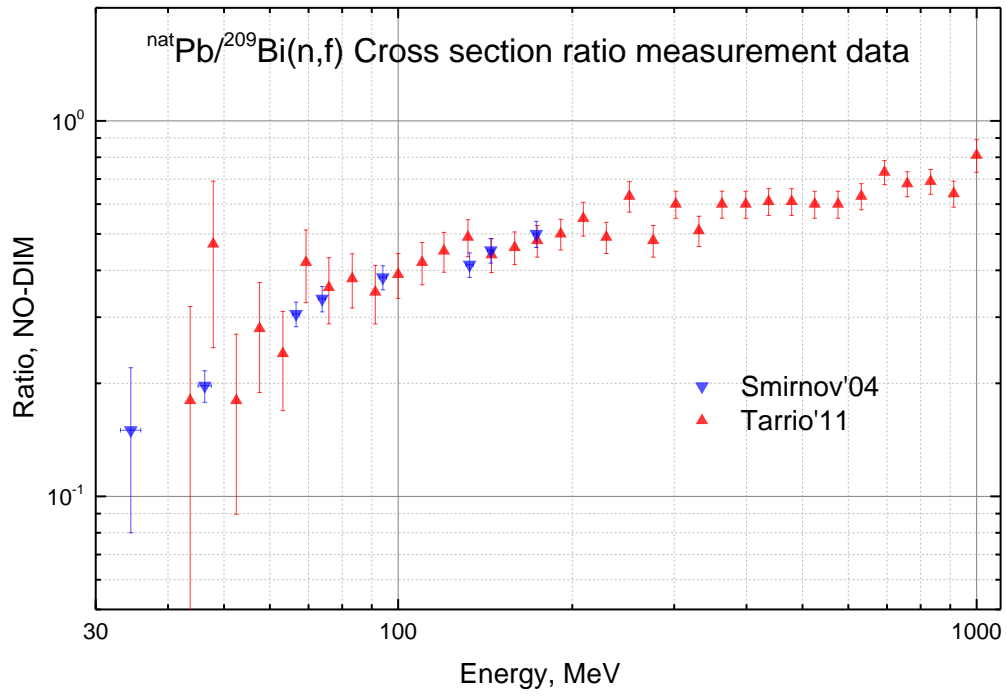
Fig. 14. Comparison of measured $^{nat}Pb/^{203}Bi(n,f)$ cross section ratio data.

APPENDIX B: Reaction Cross Section Evaluation and Parameterization

^{238}U(n,f) cross section

Fig. 15. ^{238}U(n,f) cross section: present evaluation (black curve) with usage of the scaled down (p,f) data from Kotov [33]; CEM03.03 model calculations (pink) and JENDL/HE evaluated data (green).

Table 5. ^{238}U(n,f) cross section evaluation –
recommended reference data above 200 MeV.

Energy, MeV	σ, b	Δσ,%
200	1.32	2.4
300	1.44	5.0
400	1.50	7.0
500	1.46	5.6
600	1.46	5.5
700	1.48	5.8
800	1.48	4.5
900	1.47	4.5
1000	1.47	4.6

^{235}U(n,f) cross section
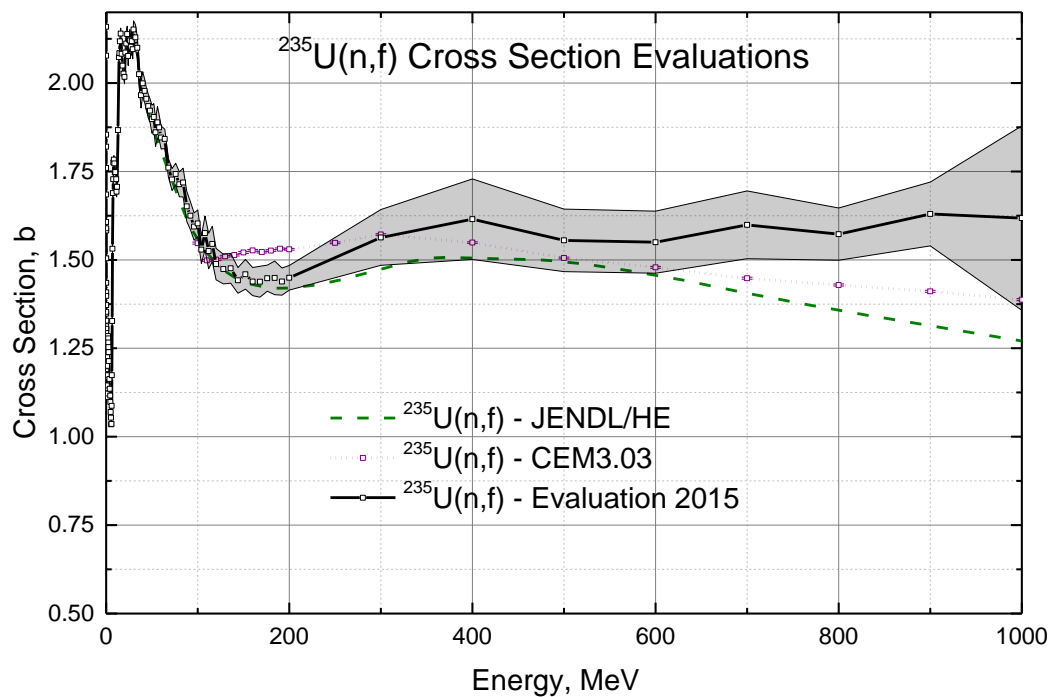
Fig. 16. ^{235}U(n,f) cross section: present evaluation (black curve) with usage of the scaled down (p,f) data from Kotov [33]; CEM03.03 model calculations (pink) and JENDL/HE evaluated data (green).
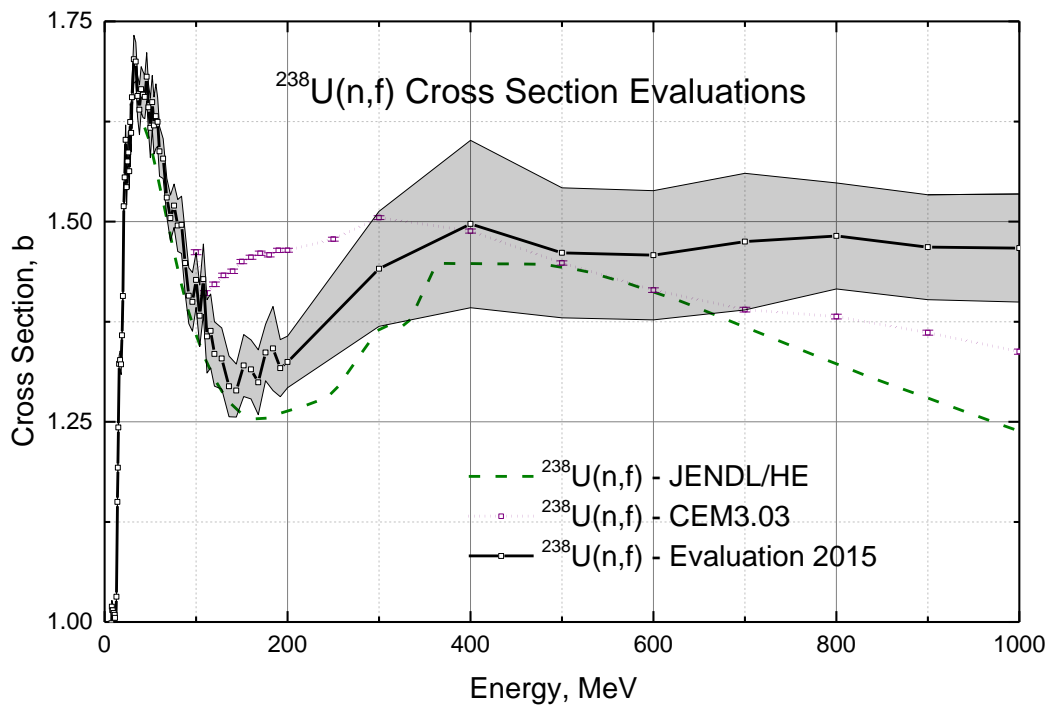
Table 6. ^{235}U(n,f) cross section evaluation –
recommended reference data above 200 MeV.

Energy, MeV	σ, b	Δσ,%
200	1.45	2.4
300	1.56	5.0
400	1.62	7.1
500	1.56	5.7
600	1.55	5.7
700	1.60	6.0
800	1.57	4.7
900	1.63	5.5
1000	1.62	16.1

^{209}Bi(n,f) cross section

The parameterization formulas were taken from previous evaluations [12, 3]. The fit was performed in two energy ranges using Origin 9.0 [34] program and statistical data weighting:

$\sigma = P_1 * e^{-\left(\frac{P_2}{x}\right)^{P_3}}$ for energies 34 to 76 MeV.

The parameterization formula was taken from [12].

Parameters: $P_1 = 62.4 \pm 11$; $P_2 = 94.1 \pm 8.6$; $P_3 = 1.63 \pm 0.13$; Fit residual $Adj. R - Square = 0.997$.

$\sigma = B * \left(1 - e^{(-A*x-C)}\right)$ for energies from 76 to 1000 MeV.

The parameterization formula was taken from previous evaluation [3].

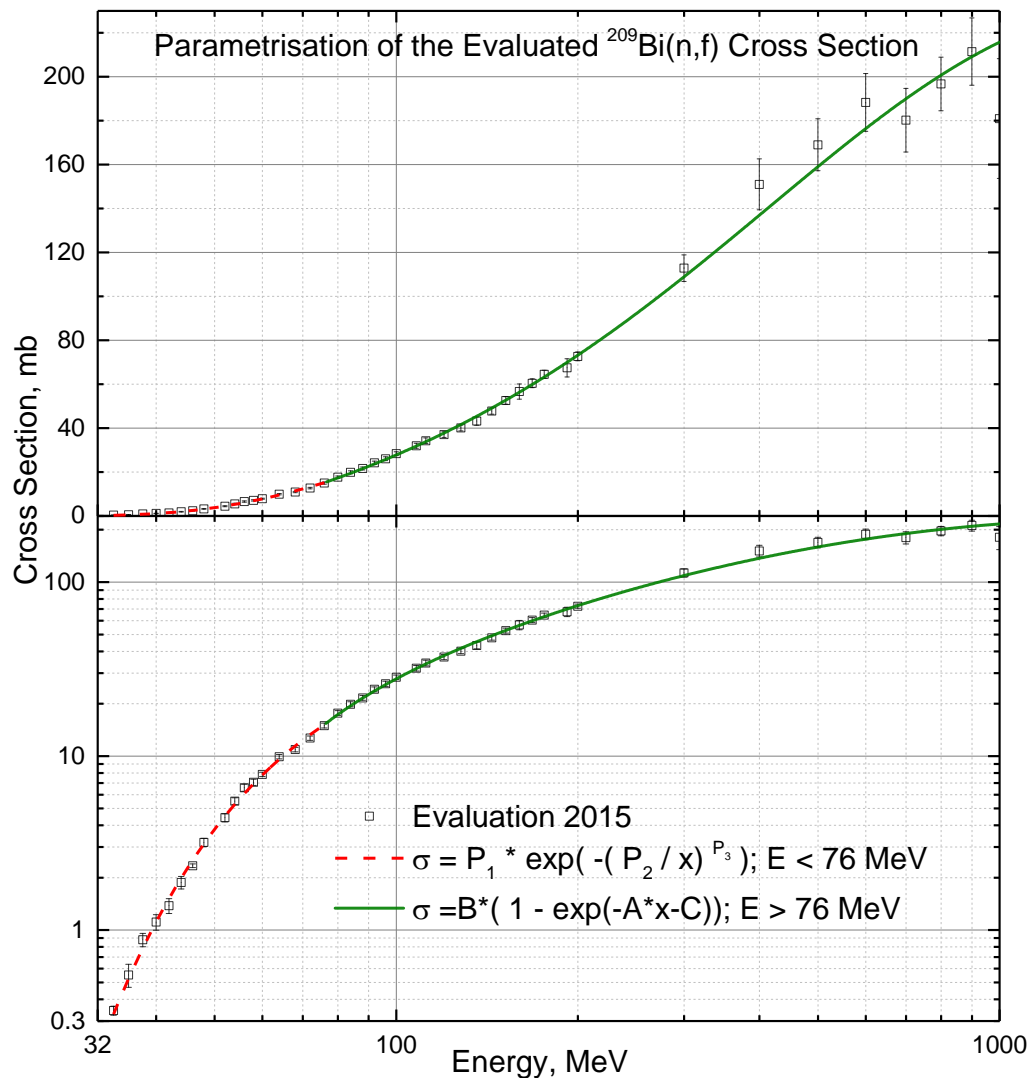Parameters: $A = 0.0024 \pm 0.0001$; $B = 240 \pm 10$; $C = -0.118 \pm 0.007$; Fit residual $Adj. R - Square = 0.997$

Fig. 17. ^{209}Bi(n,f) cross section evaluation – recommended reference data (points) and parameterization (curves) in linear (top) and logarithmic (bottom) scales.

Table 7. ^{209}Bi(n,f) cross section evaluation - recommended reference data.

Energy, MeV	σ, b	Δσ, %	Energy, MeV	σ, b	Δσ, %	Energy, MeV	σ, b	Δσ, %
34	3.44E-04	6.0	72	1.27E-02	2.9	160	5.66E-02	6.2
36	5.52E-04	15.2	76	1.50E-02	3.2	168	6.04E-02	3.4
38	8.78E-04	8.8	80	1.77E-02	3.2	176	6.45E-02	2.8
40	1.11E-03	10.3	84	1.98E-02	3.3	192	6.74E-02	6.1
42	1.38E-03	9.9	88	2.16E-02	3.2	200	7.27E-02	2.7
44	1.87E-03	8.2	92	2.42E-02	3.2	300	1.13E-01	5.4
46	2.34E-03	2.4	96	2.60E-02	3.4	400	1.51E-01	7.7
48	3.18E-03	5.4	100	2.84E-02	3.1	500	1.69E-01	7.0
52	4.42E-03	5.4	108	3.19E-02	3.6	600	1.88E-01	7.0
54	5.50E-03	4.6	112	3.43E-02	3.7	700	1.80E-01	8.1
56	6.57E-03	4.7	120	3.71E-02	3.5	800	1.97E-01	6.2
58	7.06E-03	4.1	128	4.01E-02	3.3	900	2.11E-01	7.3
60	7.84E-03	2.9	136	4.32E-02	4.4	1000	1.81E-01	15.1
64	9.91E-03	3.0	144	4.78E-02	2.9			
68	1.09E-02	3.0	152	5.26E-02	3.3			

$^{nat}Pb(n,f)$ cross section

The parameterization formulas used were taken from [12]. The fit was performed in two energy ranges using Origin 9.0 program:

$\sigma = P1 * e^{-(P2/x)^{P3}}$ for energies 34 to 84 MeV.
Parameters: $P_1 = 36.4 \pm 8.5$; $P_2 = 113.3 \pm 12.2$; $P_3 = 1.63 \pm 0.14$; Fit Residual $Adj. R - Square = 0.996$

$\sigma = P1 * e^{-(P2/x)^{P3}}$ for energies from 84 to 1000 MeV.
Parameters: $P_1 = 275 \pm 16$; $P_2 = 498 \pm 42$; $P_3 = 0.735 \pm 0.029$; Fit residual $Adj. R - Square = 0.997$
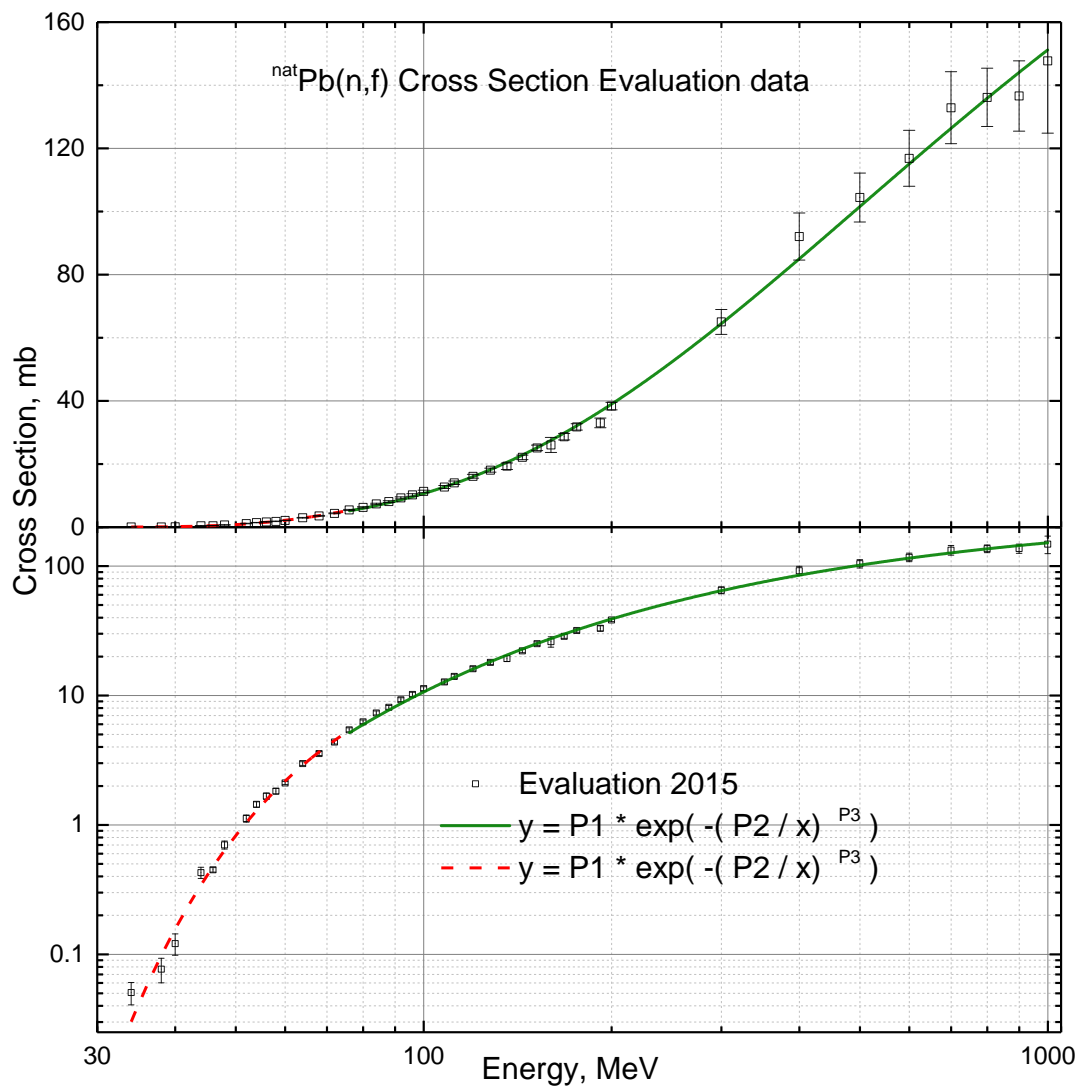

Fig. 18. ^{nat}Pb(n,f) cross section evaluation – recommended reference data (points) and parameterization (curves) in linear (top) and logarithmic (bottom) scales.

Table 8. ^{nat}Pb(n,f) cross section evaluation – recommended reference data.

Energy, MeV	σ, b	Δσ, %	Energy, MeV	σ, b	Δσ, %	Energy, MeV	σ, b	Δσ, %
34	5.05E-05	19.6	72	4.36E-03	3.3	160	2.60E-02	9.2
36	7.66E-05	21.5	76	5.43E-03	3.5	168	2.86E-02	3.6
38	1.21E-04	18.8	80	6.26E-03	3.4	176	3.17E-02	3.1
40	4.27E-04	9.9	84	7.33E-03	3.6	192	3.30E-02	4.6
42	4.48E-04	4.1	88	8.09E-03	3.5	200	3.83E-02	3.1
44	6.99E-04	7.2	92	9.27E-03	3.5	300	6.50E-02	6.0
46	1.12E-03	6.5	96	1.02E-02	3.8	400	9.20E-02	8.1
48	1.44E-03	4.7	100	1.13E-02	3.4	500	1.04E-01	7.4
52	1.67E-03	5.5	108	1.27E-02	3.8	600	1.17E-01	7.6
54	1.82E-03	4.9	112	1.40E-02	4.0	700	1.33E-01	8.6
56	2.10E-03	2.8	120	1.61E-02	3.7	800	1.36E-01	6.8
58	2.98E-03	3.2	128	1.80E-02	3.5	900	1.37E-01	8.1
60	3.56E-03	3.5	136	1.93E-02	5.2	1000	1.48E-01	15.5
64	5.05E-05	19.6	144	2.21E-02	3.2			
68	7.66E-05	21.5	152	2.51E-02	3.5			

References

[1] R. K. S. Peggs, "ESS Technical Design Report", 2013.

[2] A. Stankovskiy, E. Malambu, G.V.D. Eynde and C. Díez, "Nuclear Data Needs for the Neutronic Design of MYRRHA Fast Spectrum Research Reactor", Nuclear Data Sheets **118**, 513, 2014.

[3] A. Carlson, S. Chiba, F. Hambsch, N. Olsson and A. Smirnov, "Update To Nuclear Data Standards For Nuclear Measurements", INDC(NDS)-0368, IAEA, Vienna, May, 1997.

[4] V.I. Goldanskiy, E.Z. Tarumov and V.S. Penkina, "Heavy Nuclei Fission By the High Energy Neutrons", Doklady Akademii Nauk. **101**, 1027, 1955.

[5] P. Vorotnikov and L. Larionov, "Neutron Fission Cross Section for Bi and Pb Nuclei", Sov. J. Nucl. Phys. **40**, 552, 1984.

[6] V.P. Eismont, A.V. Prokofyev, A.N. Smirnov, K. Elmgren, J. Blomgren, H. Conde, J. Nilsson, N. Olsson, T. Ronnqvist and E. Traneus, "Relative and absolute neutron-induced fission cross sections of ^{208}Pb, ^{209}Bi, and ^{238}U in the intermediate energy region", Phys. Rev. C **53**, 2911, 1996.

[7] V. Eismont, A. Prokofiev, A. Smirnov, K. Elmgren, J. Blomgren, H. Conde, J. Nilsson, N. Olsson, T. Roennqvist, E. Traneus and P. Renberg, "Measurement of the neutron-induced fission cross sections of ^{209}Bi at 45 and 73 MeV", in *Conf. on Accel. Driven Transmut. Tech. Appl.*, Kalmar, vol. 2, p. 681, 1996.

[8] P. Staples, P. Lisowski and N. Hill, "Fission Cross Section Ratios of natPb and ^{209}Bi Relative to ^{235}U for Neutron Energies from Threshold to 400 MeV", Bull. Am. Phys. Soc. **40**, 962, 1995.

[9] O. Shcherbakov, A. Donets, A. Evdokimov, A. Fomichev, T. Fukahori, A. Hasegawa, A. Laptev, V. Maslov, G. Petrov, Y. Tuboltsev and A. Vorobiev, "Neutron-induced Fission Of ^{233}U, ^{238}U, ^{232}Th, ^{239}Pu, ^{237}Np, ^{nat}Pb and ^{209}Bi Relative To ^{235}U In The Energy Range 1-200 MeV", Nucl. Sci. Technology Suppl.*, vol. 2, no. 1, 230, 2002.

[10] A. Laptev, A. Donets, V. Dushin, A. Fomichev, A. Fomichev, R.C.Haight, O.A. Shcherbakov, S.M. Soloviev, Yu.V. Tuboltsev, A. Vorobiev, R. Haight and A. Carlson, "Fast Neutron-Induced Fission of Some Actinides and Sub-Actinides", in *Proc. 4th. Intern. Conf. Fission and Properties of Neutron-Rich Nuclei*, 2008.

[11] A.V. Fomichev, V.N. Dushin, S. M. Soloviev, A.A. Fomichev and S.G. Mashnik, "Fission Cross Sections of 240-Pu, 243-Am, 209-Bi, nat-W Induced by Neutrons up to 500 MeV Measured Relative to 235-U", Los Alamos National Labratory, 2005.

[12] A. Smirnov, V. Eismont, N. Filatov, J. Blomgren, H. Conde, A. Prokofiev, P. Renberg and N. Olsson, "Measurement of neutron-induced fission cross section for ^{209}Bi, ^{nat}Pb, ^{208}Pb, ^{197}Au, ^{nat}W and ^{181}Ta in the intermediate energy region", Phys. Rev. C **70**, 54603, 2004.

[13] A. Fomichev, V. Dushin, S. Soloviev, A. Fomichev and S. Mashnik, "Neutron Induced Fission Cross Sections for ^{240}Pu, ^{243}Am, ^{209}Bi, ^{nat}W measured relative to ^{235}U in the energy range 1-350 MeV", V.G. Khlopin Radium Institute, Saint-Petersburg RI-262, 2004.

[14] I. Ryzhov, G. Tutin, V. Eismont, A. Mitryukhin, V. Oplavin, S. Soloviev, J. Blomgren, P. Renberg, J. Meulders, Y. El-Masri, T. Keutgen, R. Prieels and R. Nolte, "Measurements of neutron-induced fission cross-sections of ^{205}Tl, ^{204,206,207,208}Pb and ^{209}Bi with a multi- section Frisch-gridded ionization chamber", Nucl. Instrum. Methods Phys. Res. Sect. A **562**, 439, 2006.

[15] R. Nolte, M. Allie, F. Brooks, A. Buffler, V. Dangendorf, J. Meulders, H. Schuhmacher, F. Smit, M Weierganz and S. Roettger, "Cross Sections for Neutron-Induced Fission of ^{235}U, ^{238}U, ^{209}Bi, and ^{nat}Pb in the Energy Range from 33 to 200 MeV Measured Relative to n-p Scattering", Nucl. Sci. Eng. **156**, 197, 2007.

[16] D. Tarrio, L. Tassan-Got, L. Audouin and B. Berthier, "Neutron-induced fission cross section of [nat]Pb and [209]Bi from threshold to 1 GeV: An improved parametrization", Phys. Rev. C **83**, 044620, 2011.

[17] V. Pronyaev, A. Carlson and R. Capote Noy, "Toward a New Evaluation of Neutron Standards", INDC(NDS)-0641, IAEA, 2013.

[18] V.P. Dzhelepov, B.M. Golovin and Y.M. Kazarinov, Institute of Nuclear Problems, Moscow, 1950.

[19] A. Reut, G. Selivanov and V. Yuriev, Institute of Nuclear Problems report, Moscow, 1950.

[20] E. Kelly and C. Wiegand, "Fission of Elements from Pt to Bi by High Energy Neutrons", Phys. Rev. **73**, 1135, 1948.

[21] T. Fukahori and S. Pearlstein, in Proceedings of the Advisory Group Meeting Organized by the IAEA, INDC(NDS)-245, edited by N.P. Kocherov ,IAEA, 1990.

[22] "jendl-he-2007", Available: http://wwwndc.jaea.go.jp/ftpnd/jendl/jendl-he-2007.html.

[23] "ROSFOND-2010", Available: http://www.ippe.ru/podr/abbn/libr/rosfond.php.

[24] E. Kim, T. Nakamura, A. Konno, Y. Uwamino, N. Nakanishi, M. Imamura, N. Nakao, S. Shibata and S. Tanaka, "Measurements of neutron spallation cross-sections", Nucl. Sci. Eng. **129**, 209, 1998.

[25] V. Bychkov and A. Pashchenko, Cross section of thershold reactions caused by neutrons, Moscow: Energoatomizdat, 1982.

[26] R. Arndt, "Nucleon-Nucleon Elastic Scattering Analysis at VPI&SU", NEANDC-205'U', Uppsala, 1991.

[27] "International Evaluation of Neutron Cross-Section Standards", IAEA, Vienna, 2006.

[28] T. Goorley, M. James, T. Booth, F. Brown, J. Bull, L.J. Cox, J. Durkee, J. Elson, M. Fensin, R.A. Forster, J. Hendricks, H.G. Hughes, R. Johns, B. Kiedrowski, R. Martz, S. Mashnik, G. McKinney, D. Pelowitz, R. Prael, J. Sweezy, L. Waters, T. Wilcox and T. Zukaitis, "Initial MCNP6 Release Overview", vol. 180, p. 298, 2012.

[29] A. Koning, S. Hilaire and S. Goriely, TALYS - 1.6 User Manual, Nuclear Research and Consultancy Group, 2013.

[30] S. Mashnik, A. Sierk and R. Prael, "MCNP6 Fission Cross Section Calculations at Intermediate and High Energies", Nuclear Data Sheets **118**, 320, 2014.

[31] E.M. Rastopchin, S.I. Mul'gin, Yu.B. Ostapenko, V.V. Pashkevich, M.I. Svirin and G.N. Smirenkin. "Statistical and dynamical aspects of preactinide fissility", Yad. Fiz. **53**, 1991.

[32] C.Paradela, M. Calviani, D. Tarrio and e. al., "High accuracy determination of the [238]U/[235]U fission cross section ratio up to ~1 GeV at n_TOF at CERN", Phys. Rev. C **91**, 2015.

[33] A.A. Kotov, L.A. Vaishnene, V.G. Vovchenko, Y.A. Gavrikov, V.V. Poliakov, M.G. Tverskoy, O.Y. Fedorov, Y.A. Chestnov, A.I. Shchetkovskiy, A.V. Shvedchikov, A.Y. Doroshenko and T. Fukahori, "Energy dependence of proton induced fission cross sections for heavy nuclei in the energy range 200-1000 MeV", Phys. Rev. C **74**, 34605, 2006

[34] Origin (OriginLab, Northampton, MA).